Perception Based Hardcopy Banding Metric

Yousun Bang, Zygmunt Pizlo and Jan P. Allebach, Purdue University, West Lafayette, Indiana, USA;
Norman Burningham, Hewlett-Packard Company, Boise, Idaho, USA

Abstract

Printer banding artifacts have been studied and analyzed by many researchers. However, banding reduction still remains an important image quality topic in the printing industry. A knowledge of how banding is perceived by human observers is vital information in designing improved new products.

In this paper we develop an analytical tool for modeling perceived banding based on human perception. We describe new Cross-platform experiments using 10 different laser printers having different imaging characteristics, and we analyze banding of the ten printers with line screen patterns. We employ pulse width modulation capability to match the absorptance of the printers, and to also generate extrinsic banding signals.

The experimental results identify the points of subjective equality of the ten printers relative to the banding of a reference printer, and provide the basis of a method of computing banding power by considering a contrast sensitivity function. Our results show that regardless of different banding spectral characteristics, the contrast banding power of a given printer can be mapped to the contrast banding power of one reference printer with added extrinsic banding. This implies that using our technique, we can reliably estimate the perceived amount of banding in a printer.

Introduction

Banding, which usually appears as nonuniform light and dark lines across a printed page, is an important quality issue in the printing industry. Many researchers have so far tried to find answers to the following questions: First, what causes printer banding?[1-3] Second, how can banding be measured or modeled?[4-6] Third, how visible is banding to observers?[7-9] Finally, how do we reduce banding?[10,11] In the above four categories of banding study, a considerable amount of work has been reported. However, no simple answers have yet been found.

A major source of difficulty is the fact that different printers have very different characteristics of banding. Depending on printer engines, printing systems, or product model numbers, the amount of banding and the frequencies of banding are quite different. The question is how can we obtain a general banding metric which can apply for all printer models. Once we have it, it will provide a very helpful guide in designing a new printer with reduced banding.

So far no literature has reported comparison results of banding levels in different printers. In this paper, we design a novel Cross-platform experiment using 10 different monochrome laser printers having different banding spectral contents, compare the levels of banding, and then establish a banding metric which reliably estimates the amount of perceived banding for each printer. Our approach is to measure the amount of perceived banding for each of the 10 printers by finding an equivalent level for one fixed printer. In their previous work,[9] the authors described a methodology for measuring an observer's ability to discriminate between images having different levels of banding for a given printer. To control banding levels, an α-level of extrinsic banding was added to the printer intrinsic banding. We will employ a similar methodology to measure the visibility of banding across different printers. However, comparing the banding levels of different printers involves two important considerations.

First, we must take into account the influence of the halftone patterns of different printers. Each printer has its own halftone patterns; and it is well known that screen angles, screen frequencies, or dot arrangements are strongly correlated to the visibility of banding. Therefore, we should control the effect of halftone patterns by applying the same pattern to all 10 of the printers. Second, we also need to consider tone dependency of banding visibility. Thus, we should properly calibrate the printers to compare the same tones of images. In the paper, we use line screen patterns and the pulse width modulation capability of one printer to solve the above problems.

The rest of the paper is organized as follows. In the next section, we describe our framework for the 10-printer experiments, and show how we generate test samples. Then we present the procedures for the psychophysical Cross-platform experiments. Finally we discuss our experimental results and draw some conclusions.

Framework of 10-Printer Experiments

To obtain a reliable banding metric, we design psychophysical experiments using ten different printers with different spectral characteristics. The ten monochrome laser printers having various levels of intrinsic banding were carefully chosen for our experiments: They are made by six different manufacturers, and range from very low-end to high-end market segments for monochrome laser printers. When we measure visibility of banding with different printers, we want to avoid having the role of the halftoning algorithm influence our results. We will show how we designed the test patch for our experiments to achieve this objective.

Test Patch Design with Line Patterns

We design a special test patch consisting of lines parallel to the paper process direction. Since banding occurs in the direction perpendicular to the paper process direction, we do not want the line patterns to influence banding visibility. With each of the ten test printers, we use the same [0,1,1,0,0] repeated line pattern, where 0 is white, and 1 is black. This is illustrated in Fig. 1 where

the zoomed area shows 4 repeated [0,1,1,0,0] line patterns. When we print this patch using the ten printers, each printed patch appears uniform gray at a 12 inch normal viewing distance, ignoring banding and other potential artifacts. We measured the luminance CIE Y values of the 10 patches with a spectrophotometer.[†] The options of "absolute white", "D65 light", and "no filter" were selected to calibrate a white point using the "SPM 50 standard target". The measured luminance Y values vary from 22.03 to 37.82 as shown in Table 1.

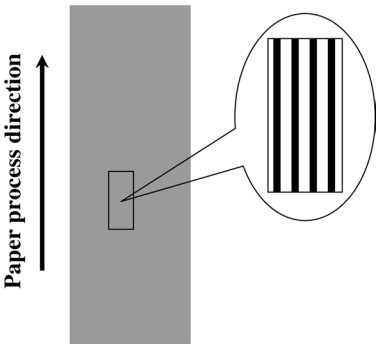

Figure 1. Test patch having the 01100 line pattern.

Table 1: Average Gretag Y Value of [0,1,1,0,0] and tone Matched Baseline Pattern of Printer A.

Test Printer	Average Y Luminance	Baseline Pattern
Printer 1	29.28	[1 63 63 1 0]
Printer 2	22.18	[21 63 63 21 0]
Printer 3	22.24	[21 63 63 21 0]
Printer 4	22.69	[21 63 63 21 0]
Printer 5	26.56	[8 63 63 8 0]
Printer 6	30.77	[0 54 54 0 0]
Printer 7	37.82	[0 38 38 0 0]
Printer 8	24.30	[15 63 63 15 0]
Printer 9	24.51	[15 63 63 15 0]
Printer 10	22.03	[21 63 63 21 0]

We then select the reference printer[‡] *Printer A*. Our aim is to measure the perceived amount of intrinsic banding of the test printers by identifying the equivalent amounts of extrinsic banding for Printer A. Therefore for Printer A we picked the printer which showed the lowest level of banding compared to each of the ten printers. Then we could add extrinsic banding to the intrinsic banding of Printer A for the comparison with each of the test printers. In the following sections, we will describe how we matched the absorptance between Printer A and each test printer, and also show how to generate the extrinsic banding signal for each test printer.

Calibration of Line Patterns and Absorptance Match

Because of the tone dependency of banding visibility, we should match the absorptance when comparing the banding levels of two different printers. By using the pulse width modulation (PWM) capability of Printer A, we vary the tone of Printer A to match the absorptance of the test printer that is obtained when we print the fixed 01100 pattern. Printer A accepts an 8 bit PWM code for each pixel. Six bits control the pulse-width and two bits determine the pulse justification. With this, each pixel can have 64 gray levels from 0 (white) to 63 (black), and can be left, center, right, or split justified.

For the exact tone match, we need to perform a calibration process of Printer A with the line patterns. To do this, we designed 1273 in. × 7 in. gray test patches having repeated line patterns of the form [0, *x, x*, 0, 0] or [*y*, 63, 63, *y*, 0], where *x* and *y* are gray values between 0 and 63. In order to make the PWM printing more stable, we used the justification codes shown in Table 2. In the table, R, L, and C stand for right, left, and center justification, respectively. For convenience, we now represent our PWM codes by *P* where

$P = x$, if line pattern is of the form of [0, *x, x*, 0, 0]
or $P = y + 63$, if it is of the form of [*y*, 63, 63, *y*, 0].

Table 2: Justification modes used for Our Test Patch Design.

Pulse Width Code	Pulse Justification Code (Right, Left, Center)
[0, *x, x*, 0, 0]	[-,R,L,--,]
[*y*, 63, 63, *y*, 0]	[R,C,C,L,-]

We printed the test pages at the default resolution of 600 dpi. We then measured the luminance Y values of the patches using the spectrophotometer. Since there were small variations within each printed patch, we measured the values at 5 different locations along the patch and took the average value. The measured calibration curve is shown in Fig. 2. The plot shows that the measured Y values decrease smoothly as *x* and *y* increase from 0 to 63 in the line patterns of the form [0, *x, x*, 0, 0] and [*y*, 63, 63, *y*, 0].

By applying the inverse of this calibration curve to the luminance Y value of the printed 01100 patch for each test printer, we obtain the corresponding line pattern which produces the same absorptance for Printer A. In this paper, we will call this tone-matched line pattern the *baseline pattern* for the test printer. Table 1 shows the average Y values and the corresponding baseline patterns of Printer A for the 10 test printers. We then use test patches with these line patterns for our banding experiments. For example, we use the test patch with [1, 63, 63, 1, 0] repeated line patterns for the experiment between Printer 1 and Printer A.

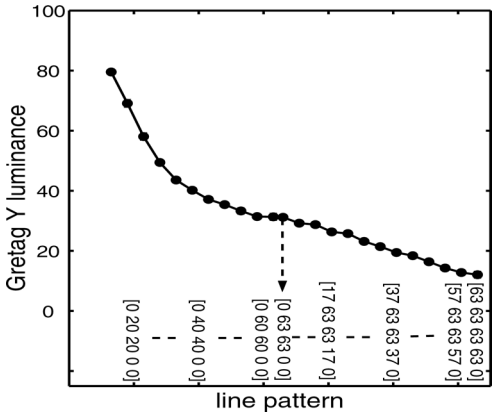

Figure 2. Measured Gretag Y luminance vs. corresponding line patterns.

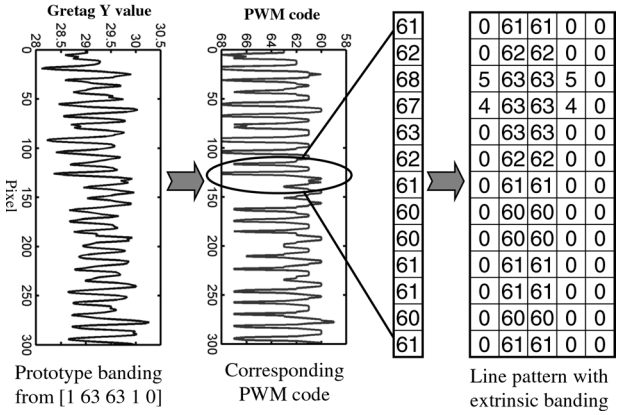

Figure 3. The modulation process for generating a test patch with extrinsic banding.

Modulation Process For Extrinsic Banding

To generate various levels of extrinsic banding for Printer A, for each test patch printed with the tone matched line pattern using Printer A, we extract a one dimensional prototype banding signal. To do this, we employ the method described in the paper by Bang et al.[9] We filter the 1-D banding signal in the spatial domain using a 5th order Butterworth bandpass filter with the cutoff frequencies 1 cycles/in and 200 cycles/in. We then apply the scanner calibration curves to obtain the 1-D prototype banding signals in units of Gretag Y luminance. To prevent phase from affecting the results of experiments, we randomly shift the phase of the extrinsic banding signal whenever we print the image with extrinsic banding.

For the banding level α, we multiply the amplitude of the prototype banding signal by α to obtain an α−level extrinsic banding signal. Here, α depends on the baseline pattern. The value $\alpha = 0$ means no extrinsic banding is added; and $\alpha = 1$ means that the amount of extrinsic banding added is the same as that of the intrinsic banding. Next, we apply a calibration curve which is the inverse of the curve shown in Fig. 2 to the α-level extrinsic banding signal, and convert the values into the PWM codes *P*. Then we expand the PWM codes to the corresponding line patterns in the direction perpendicular to the lines. In Fig. 3, the modulation process of the line patterns is illustrated. The array on the far right side shows the image with an extrinsic banding signal. Therefore, for a given α we can generate an image with an extrinsic banding signal by using the pulse codes.

Psychophysical Cross-platform Experiments

For each of the 10 test printers, we created print samples with both intrinsic and extrinsic banding using Printer A. We carefully selected the range of banding level α for each test printer. Since all ten printers have different levels of banding, the ranges of α chosen varied from printer to printer. We used the method of constant stimuli in our Cross-platform experiments. For each session, test stimuli with 8 levels of α were used. Using five different prints for each banding level, each subject did a total of 40 trials for each session. In the method of constant stimuli, on each trial the reference print from the test printer and various levels of test stimuli from Printer A were presented to the subject. The reference print contained only intrinsic banding of the test printer, and the test prints contained intrinsic plus extrinsic banding of Printer A. The level of the test stimulus varied randomly from trial to trial.

We used mat boards[§] for our experiments and mounted all the prints on the boards. We used the regular mat with neutral color *Crescent 934 Pearl* for the core (outer mat size: 10 in. × 13 in., opening size: 7.5 in. × 10 in) and white regular mat for backing. We put the image labels on the mounted prints by assigning a randomly generated integer.

For each test printer, 13 to 15 Purdue graduate students participated in our experiments. The subject's task was to say whether the test image had more or less banding than the reference print. Subjects recorded their answers on a computer. By analyzing the subjects' responses, we measured the probabilities that the subjects discriminated between the reference print and the test stimuli. Since a perceptual Gaussian model is widely accepted in psychophysics, of visible banding, we adjusted the ranges and intervals of α we conducted a Probit analysis to fit a normal cumulative for the experiments depending on the test printers. function to our data.[12] We also estimated psychometric functions of the subjects for the each test printer, and then ob tained an equivalent banding level of Printer A for each test printer. This equivalent level is called *the point of subjective equality* (PSE), and each subject's PSE can be estimated by the mean value of the fitted cumulative Gaussian function. In the next section, we will present our experimental results.

Results and Discussion

For each of the 10 test printers, we obtained psychometric functions for all the subjects by conducting a series of Probit analyses. Figure 4 shows the estimated psychometric functions for Printer 2. Each subject's data produced a smooth psychometric function, and they were all well fitted to Gaussian functions.

We computed the average PSE and the standard error for each test printer. The standard error is the estimated standard variation of the average PSE. The measured average PSE for each test printer is the banding level of Printer A at which an average subject sees that the intrinsic banding of the test printer is perceptually

equivalent to that of the reference printer. Table 3 shows the obtained average PSE for each test printer. Among the 10 printers, Printer 9 had the lowest PSE, and Printer 7 had the highest PSE, which was greater by a factor of 4.98. This shows that the visibility of banding varies significantly from printer to printer. As we mentioned earlier, since each test printer has a different level of visible banding, we adjusted the ranges and intervals of α for the experiments depending on the test printers.

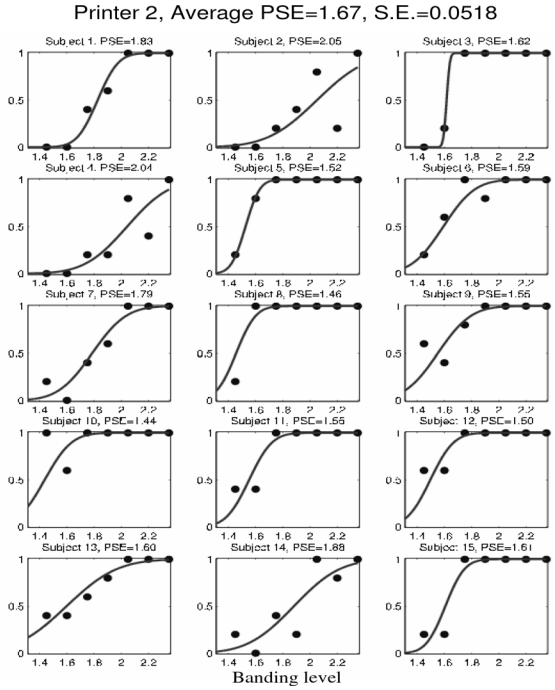

Figure 4. Estimated psychometric functions for Printer 2.

Table 3: Average PSE with Standard Error and Banding Levels Used

Test Printer	Average PSE	α Levels Used
Printer 1	1.53 (± 0.053)	0.60 − 2.70
Printer 2	1.67 (± 0.052)	1.30 − 2.35
Printer 3	0.81 (± 0.027)	0.50 − 1.20
Printer 4	1.23 (± 0.055)	0.90 − 1.81
Printer 5	1.05 (± 0.056)	0.60 − 1.65
Printer 6	0.65 (± 0.035)	0.30 − 1.00
Printer 7	2.54 (± 0.083)	2.00 − 3.40
Printer 8	0.80 (± 0.045)	0.50 − 1.41
Printer 9	0.51 (± 0.066)	0.24 − 1.36
Printer 10	1.30 (± 0.079)	0.75 − 1.80

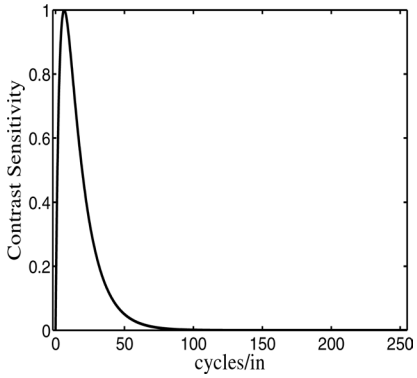

Figure 5. Campbell's contrast sensitivity function at a 12 inch viewing distance.

Regardless of the different spectral contents, the subjects successfully performed the experiments, and they were all able to compare the banding levels of the two different printers. After obtaining the PSE's for the 10 printers, we generated the test patches for Printer A with extrinsic banding signals of those PSE levels. We printed them using Printer A; and we visually confirmed that they had a level of banding that is perceptually equivalent to the intrinsic banding of the test printers.

In order to establish a banding metric, we measured and compared the banding power of the intrinsic banding of the 10 test printers and Printer A with the obtained PSE's. The method of computing banding power is described in the authors' previous work.[9] Since banding perception depends on the contrast of an image, we applied Campbell's contrast sensitivity function (CSF) to the banding spectra. Figure 5 shows Campbell's CSF at a 12 inch viewing distance. Then, we normalized the banding power of the test printers by the reflectance squared to obtain the contrast banding power.

The banding signals associated with laser EP printers have a complex structure that varies significantly among different printer models. This can be seen in the left column of Fig. 6 which shows spectral plots for the 10 printers that we investigated in this paper. In general, the banding spectra consist of one or more strong, distinct spectral lines against a broadband background of continuous spectral power. The distinct spectral lines are perceived as perfectly periodic bands superimposed on top of an irregular pattern that varies only in the process direction. In our earlier work, we found that for a single printer, the banding visibility scaled linearly with the power of the banding signal, integrated over a broad passband.[9] However, for the data obtained from the 10 printers, we found that this was no longer the case. In particular, banding signals with strong, isolated high frequency components were less visible than would be predicted on the basis of their integrated spectral power, or the spectral power computed after normalizing the banding signal by the average gray value to yield contrast, and multiplying the banding spectrum by the HVS contrast sensitivity function for a normal viewing distance.

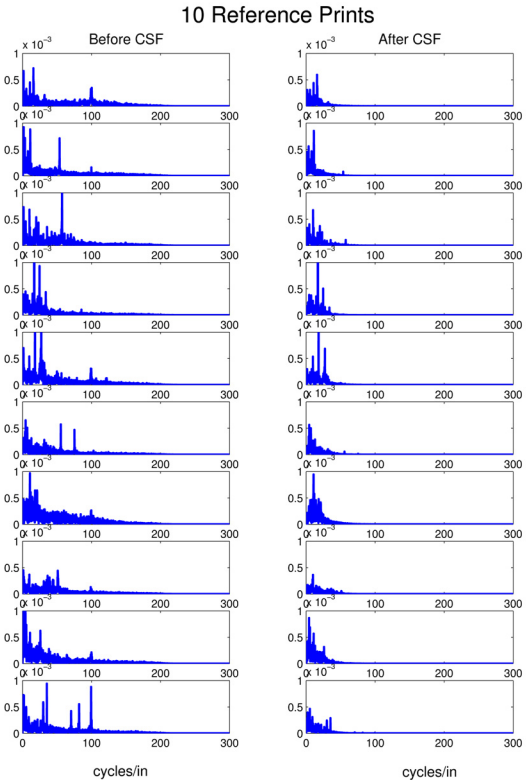

Figure 6. Spectral plots of the 10 test printers before and after applying CSF for a viewing distance of 45 inches.

We hypothesized that the viewers were "seeing through" the strongly periodic high frequency component and thereby discounting it to some extent. This behavior would be consistent with the adaptive nature of the human visual system and the anecdotal evidence that viewers can easily see through a periodic, clustered-dot halftone texture to identify image detail, even when the halftone texture is actually quite visible. As just one possible way to account for this, we investigated the concept of increasing the effective viewing distance associated with the contrast sensitivity function, thereby attenuating the high frequency components. We view the PSEs determined by our psychophysical experiments as the true measure of relative banding visibility among the 10 printers. Thus, we defined the cost function given in Eq. (1) as a measure of how well the visually weighted banding contrast power predicts PSE.

$$\Phi(d) = \sum_{i=1}^{10} \left(\frac{P^d_{A+PSE_i} / r^2_{A+PSE_i}}{P^d_{test_i} / r^2_{test_i}} - 1 \right)^2 \qquad (1)$$

Here, i is the index corresponding to the test printer, P^d is banding power after applying the CSF at a viewing distance d, r is the average reflectance of the patch, and the subscripts $A + PSE_i$ and $test_i$ stand for Printer A at the PSE for Printer i and each of the 10 test printers, respectively. This cost function depends on the viewing distance d. It is shown in Fig. 7. As can be seen there, 45 inches is the minimizing value for d. We apply the CSF with a 45 inch viewing distance to the banding spectra of the test printers. Figure 6 shows the spectra of the 10 test printers before and after applying the contrast sensitivity function at the 45 inch viewing distance.

Figure 8 shows the logarithm of the visually weighted contrast power for Printer A at the PSE versus the logarithm of the visually weighted contrast power for the test printer. The plot shows that there is a strong correlation between log contrast power of Printer A at the PSE and log contrast power of the test printers. Although the 10 test printers have different spectral characteristics, the measured contrast power of intrinsic banding in the test printers can be mapped into the contrast power of Printer A. Therefore, this implies that we can quantify the perceived banding in a given printer by measuring the corresponding contrast power of one specific printer – Printer A.

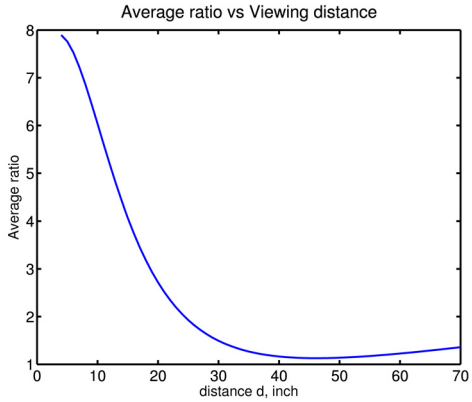

Figure 7. Average ratio of the contrast power of Printer A at the PSE to that of the the test printers vs. the viewing distance for the CSF.

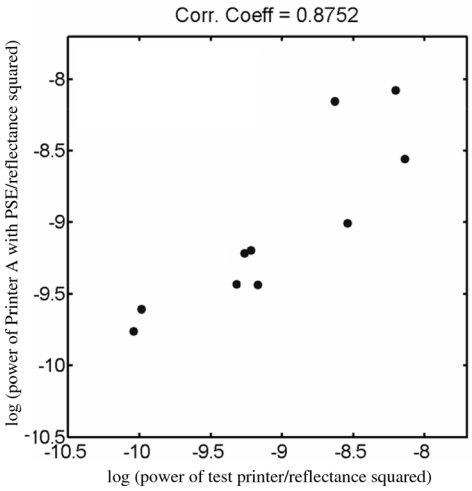

Figure 8. Log contrast power of Printer A at the PSE vs. log contrast power of the 10 test printers viewed at a distance of 45 inches.

Conclusion

In the paper, we developed a novel methodology to compare the banding levels of different printers. We quantified perceived

banding of 10 different printers by measuring the logarithmic contrast banding power. Based on our 10-printer experiments, we found that regardless of the different banding spectral contents, the contrast banding power of a given printer can be directly mapped to the contrast banding power of one reference printer with added extrinsic banding signals. This suggests that we can reliably estimate the amount of perceived banding in any laser printer, and thus our method can assist in the design of a new printer having reduced banding.

Acknowledgment

We gratefully acknowledge the support from the Hewlett Packard Company for this research, and we would like to express sincere gratitude to Kainlu Low for his assistance during this project. We also wish to thank all the subjects who participated in the experiments.

References

* Now with Samsung Advanced Institute of Technology, Giheungeup, Yonginsi, Gyeonggido, South Korea
† Gretag SPM 50: Gretag Aktiengesellschaft, Zurich,Switzerland
‡ HP LJ 9000
§ MatShop/Island Art Shop: Bellingham, WA 98226

1. D. D. Hass, Contrast modulation in halftone images produced by vibration in scanline spacing, J. Imaging Technology, 15(1), 46 (1989).
2. R. P. Loce, W. L. Lama and M. S. Maltz, Modeling vibration-induced halftone banding in a xerographic laser printer, J. Elect. Imag., 4(1), 48 (1995).
3. Je-Hwan You, Hyeong-Chae Kim and Sang-Yong Han, Banding reduction in electrophotographic printer, in Proc. IS&T's NIP20: International Conference on Digital Printing Technologies, Salt Lake City, UT, pp. 470 – 473 (2004).
4. J. C. Briggs, M. Murphy and Y. Pan, Banding characterization for inkjet printing, in Proc. IS&T's PICS: Image Processing, Image Quality, Image Capture, Systems Conference, Portland, OR, pp. 84 – 88 (2000).
5. P. J. Kane, T. F. Bouk, P. D. Burns and A. D. Thompson, Quantification of banding, streaking and grain in flat field images, in Proc. IS&T's PICS: Image Processing, Image Quality, Image Capture, Systems Conference, Portland, OR, pp. 79 – 83 (2000).
6. Woonyoung Jang and Jan P. Allebach, Simulation of print quality defects, J. Imaging Science and Technology, 49(1), 1 (2005).
7. C. Cui, D. Cao and S. Love, Measuring visual threshold of inkjet banding, in Proc. IS&T's PICS: Image Processing, Image Quality, Image Capture, Systems Conference, Montreal, Quebec, Canada, pp. 84 – 89 (2001).
8. Wencheng Wu, Edul N. Dalal and Rene Rasmussen, Perceptibility of nonsinusoidal bands, in Proc. IS&T's NIP18: International Conference on Digital Printing Technologies, San Diego, CA, pp. 462 – 466 (2002).
9. Yousun Bang, Zygmunt Pizlo and J.P. Allebach, Discrimination based banding assessment, in Proc. IS&T's NIP19: International Conference on Digital Printing Technologies, New Orleans, LA, pp. 745 – 750 (2003).
10. C. Chen and G. Chiu, Banding reduction in electrophotographic process, in Proc. IEEE/ASME Int. Conf. Advanced Intelligent Mechatronics, Como, Italy, pp. 81 – 86 (2001).
11. Guo-Yau Lin, Jimmy M. Grice, Jan P. Allebach, George T. C. Chiu, Wayne Bradburn and Jeff Weaver, Banding artifact reduction in electrophotographic printers by using pulse width modulation, J. Imaging Science and Technology, 46(4), 326.
12. D. J. Finney, Probit Analysis, Cambridge University Press, NY, 3rd ed. (1971)

Author Biography

Yousun Bang received the B.S. degree in mathematics from Ewha Womans University, Seoul, Korea, in 1994 and the M.S. degree from Purdue University, West Lafayette, IN, in 1999. She finished her Ph.D. final defense in the School of Electrical and Computer Engineering, Purdue University, West Lafayette, IN, in 2004. She has been working in Imaging Solution Program Team at Samsung Advanced Institute of Technology since 2004. Her research interests include electronic imaging systems, color image rendering and processing, and image quality.